American Mineralogist, Volume 68, pages 156–163, 1983

The 3*T*, 4*T* and 5*T* polytypes of wollastonite from Kushiro, Hiroshima Prefecture, Japan

CHIYOKO HENMI, AKIRA KAWAHARA, KITINOSUKE HENMI

Department of Earth Sciences, Faculty of Science
Okayama University, Okayama 700, Japan

ISAO KUSACHI

Department of Earth Sciences, School of Education
Okayama University, Okayama 700, Japan

AND YOSHIO TAKÉUCHI

Mineralogical Institute, Faculty of Science
University of Tokyo, Tokyo 113, Japan

Abstract

In addition to the common 1*T* and 2*M* polytypes of wollastonite, three kinds of polytypes, 3*T*, 4*T* and $5T_1$, are found at Kushiro, Hiroshima Prefecture, Japan. The long-period polytypes have the lattice constants: a = 23.2(1), b = 7.30(3), c = 7.06(3)Å, α = 90.0°, β = 95.5(2)°, γ = 94.6(2)°, a = 31.2(1), b = 7.30(3), c = 7.06(3)Å, α = 90.0°, β = 95.5(2)°, γ = 96.8(2)°, and a = 38.6(1), b = 7.30(3), c = 7.06(3)Å, α = 90.0°, β = 95.5(2)°, γ = 98.0(2)°, respectively. The stacking sequences of the 3*T*, 4*T* and $5T_1$ polytypes were determined by the diffraction intensities of *hk*0 reflections as TTG, TTTG and TTTTG, respectively. The $5T_1$ polytype found is one of the three possible 5*T* polytypes.

These polytypes occur in zone skarns consisting of a grossular zone, an idocrase zone and a wollastonite zone which were formed around andesite dikes penetrating a limestone body. The wollastonite crystals occur throughout the skarn bodies and the 2*M* to 1*T* volume ratio in the crystals decreases with increasing distances from the dike, with the wollastonite zone mostly consisting of the 1*T* polytype. The 3*T*, 4*T* and $5T_1$ polytypes were found in the idocrase zones and nearby, where both 1*T* and 2*M* coexist. Thus, the long-period wollastonite polytypes might form under the conditions intermediate between those under which the 1*T* and 2*M* polytypes formed.

Introduction

Ito (1950, p. 93–110) showed that there is a special structural relationship between wollastonite and parawollastonite. This structural relationship is, at present, treated in terms of polytypism; triclinic wollastonite and monoclinic parawollastonite are denoted as 1*T*[1] and 2*M* polytypes, respectively. No further X-ray investigation of wollastonite polytypes has been carried out, except for those concerning the so-called "4*T* wollastonite" (Wenk, 1969) and the disordered structures (Jeffery, 1953; Ueda, 1966; Jefferson and Bown, 1973). However, Takéuchi (1971) made theoretical and systematic considerations of possible polytypes of wollastonite. Henmi *et al.* (1978) reported an occurrence of the 7*T* polytype, and also suggested possible occurrences of other wollastonite polytypes in nature.

We have studied wollastonites from Kushiro, Hiroshima Prefecture, Japan, using the single crystal precession method. The diffraction spots along k = odd lattice lines in some of the precession photographs occur with regular intervals corresponding to ⅓, ¼ or ⅕ of the a^*-periodicity of 1*T* wollastonite. In the present paper, we report the results of our study concerning new modes of stacking sequences with three, four and five elementary units in wollastonite polytypes.

[1]The polytype notations of 1*T*, 2*M*, 3*T*, 4*I*, 4*M* and 5*T* in the present paper correspond to 1*TC*, 2*PM*, 3*TC*, 4*TC*, 4*PM* and 5*TC*, respectively, of Bailey (1977).

0003–004X/83/0102–0156$02.00

Notation of stacking sequences

The structural difference between triclinic wollastonite (*1T*) (Buerger and Prewitt, 1961) and monoclinic parawollastonite (*2M*) (Trojer, 1968) has been interpreted to be due to different modes of stacking of a pseudomonoclinic subcell along the direction of the *a*-axis. In order to describe wollastonite polytypes systematically, we use a slightly different notation described by Henmi *et al.* (1978), which is summarized as follows. The polytypism of wollastonite can be discussed in terms of stacking of (100) slabs, each being one unit cell thick, of the 1T wollastonite structure. Note that this is not the pseudomonoclinic subcell of previous workers. Let T denote a slab in a continuous position with respect to the preceding one and G a slab that is displaced by *b*/2. Then the *1T* polytype (triclinic wollastonite) is represented by TTT . . . or (T), and the *2M* polytype (monoclinic parawollastonite) by TGTGTG . . . or (TG). Similarly, the stacking sequence for 3*T* (3-layered structure) is given by TTGTTGTTG . . . or (TTG) which may be rewritten as (2T1G). These examples are illustrated in Figure 1. The 7*T* polytype from Fuka (Henmi *et al.*, 1978) has the stacking sequence of TTGTGTG (4T3G), which is one of the eight possible stacking sequences for 7*T* polytypes.

There are two kinds of modes in the stacking sequences having four slabs in the repeating units: the triclinic 4*T* polytype and the monoclinic 4M polytype (Fig. 3). The stacking sequence of the former is represented by (TTTG) and the latter by (TTGG). The polytypes with five slabs in the repeating units have the following three kinds of modes in the stacking sequences; TTTTG, TTTGG and TTGTG (Fig. 5). They are all triclinic and are called the 5*T* polytypes.

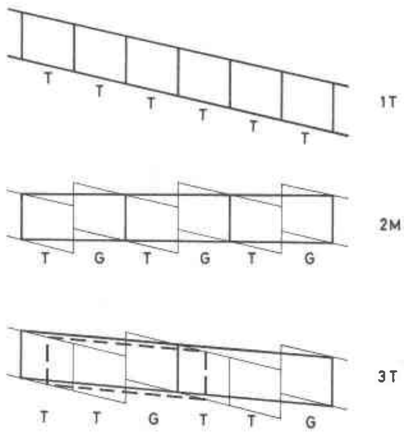

Fig. 1. The stacking sequences of (100) slabs for wollastonite polytypes. Thick lines indicate the unit cells. See text for explanation of the symbols T and G. Figure 3 of Henmi *et al.* (1978). The broken lines indicate the unit cell chosen for the space group, $P\bar{1}$, for the 3*T* polytype.

Experimental

The specimens used in this study are prismatic in shape, 0.2–0.5 mm long (along *b*), and have cross sections with dimensions of 0.1–0.3 mm. The zero-level precession photographs about *b* were recorded for each specimen using Cu$K\alpha$ radiation. The intensities of *hk*0 reflections were visually estimated in the precession photographs. For this purpose, four photographs of each specimen, showing *hk*0 reflections, were taken with different exposure times and a standard scale was prepared. The intensities were corrected for Lorentz and polarization factors and reduced to structure factors.

Calculation of structure factors

We calculated the structure factors for 3*T*, 4*T* and 5*T* polytypes with the stacking sequences shown in Figures 1, 3 and 5 respectively, using the same procedure described by Henmi *et al.* (1978). In the reciprocal k = even rows throughout all polytypic structures, the intensities of the diffraction maxima at the positions which correspond to those of the 1*T* polytype are very strong, whereas those at other positions are extremely weak. It was very difficult to measure these weak intensities by the photographic method. On the other hand, diffraction spots in the k = odd layer lattice lines in general do not overlap. Their intensities were readily measured with accuracy, and thus they were used to determine the kinds and proportions of polytypes in the specimens examined.

Results

3T polytype

The 3*T* polytype was found in five Kushiro specimens. Most of these specimens are composite crystals consisting of 3*T* and other polytypes, such as 1*T* and 2*M*, with the *Y* and *Z* directions parallel. A portion of a representative zero-level precession photograph about the *c*-axis is shown in Figure 2. The repeat interval along the *h*10 layer line is ⅓ of that determined from the *h*00 or *h*20 layer lines and ⅓ of the *a**-periodicity of the 1*T* wollastonite polytype. The calculated structure factors in the k = odd rows of the 3*T* polytype (TTG) are compared in

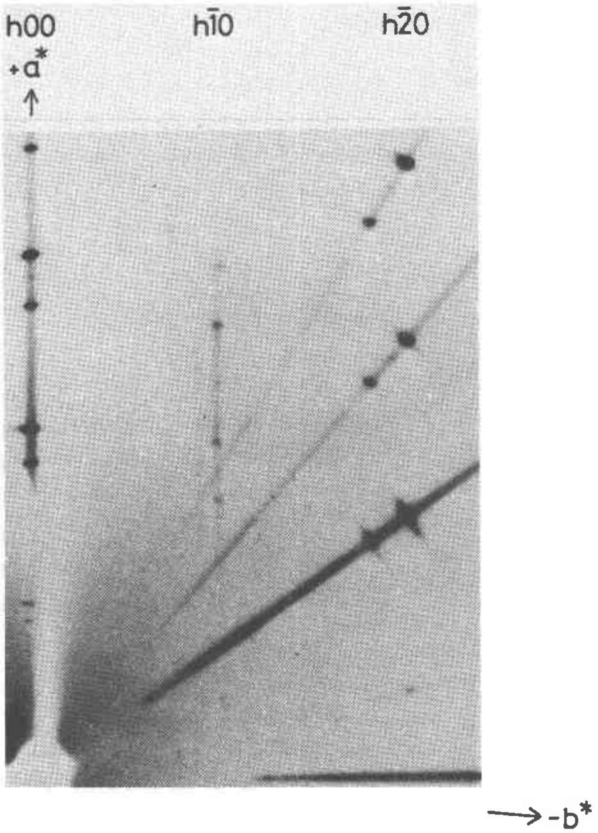

Fig. 2. Part of a precession photograph, taken about c, of 3T polytype from Kushiro. The interval of h10 reflections is ⅓ that of detectable h00 or h20 reflections and is also ⅓ of 1T wollastonite.

Table 1. Observed and calculated structure factors of the 3T wollastonite

hkl	Fo	Fc	hkl	Fo	Fc
010	0	-0.4	$3\bar{1}0$	0	2.3
110	0	1.4	$4\bar{1}0$	0	4.1
210	0	-0.1	$5\bar{1}0$	22	15.9
310	5	-5.0	$6\bar{1}0$	27	-23.1
410	14	12.0	$7\bar{1}0$	16	-13.2
510	11	9.9	$8\bar{1}0$	27	-22.1
610	27	25.5	$9\bar{1}0$	16	12.4
710	27	-25.3	$10\bar{1}0$	0	1.9
810	10	-8.7	$11\bar{1}0$	0	-2.8
910	0	-7.7	$12\bar{1}0$	10	8.8
1010	0	0.4	$13\bar{1}0$	8	6.1
1110	0	-3.0	$14\bar{1}0$	11	9.1
1210	11	-11.1			
1310	11	11.4	$5\bar{3}0$	0	3.2
1410	0	2.9	$6\bar{3}0$	0	1.7
430	0	3.5	$7\bar{3}0$	0	1.0
530	0	-2.6	$8\bar{3}0$	5	4.3
630	0	0.7	$9\bar{3}0$	8	5.9
730	5	7.8	$10\bar{3}0$	27	20.4
830	17	-16.3	$11\bar{3}0$	30	-25.5
930	8	-11.8	$12\bar{3}0$	16	-12.4
1030	24	-26.1			
1130	18	21.0			

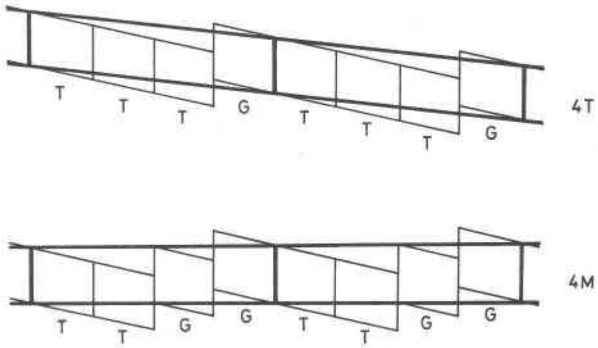

Fig. 3. The stacking sequences of 4T and 4M polytypes. The thin lines indicate the unit cells of 1T and the thick lines those of 4T or 4M.

Table 1 with observed values, giving an R value 0.25. The photograph also shows diffuse streaks parallel to a^* along the k = odd rows (Fig. 2), indicating some stacking disorder. The space group is P$\bar{1}$, and the corresponding unit cell is shown in Figure 1 by broken lines.

4T and 4M polytypes

The 4T polytype has the stacking sequence shown in Figure 3. It is easily distinguished from the other sequences by the positions of diffraction maxima in k = odd rows. These reflections have intervals ¼ of those of 1T wollastonite polytype (Fig. 4). One such specimen was found, although it proved to be a composite crystal consisting of 1T and 4T polytypes. The diffraction intensities for 4T were weak because, for this crystal, its proportion by volume was relatively small, and hence the

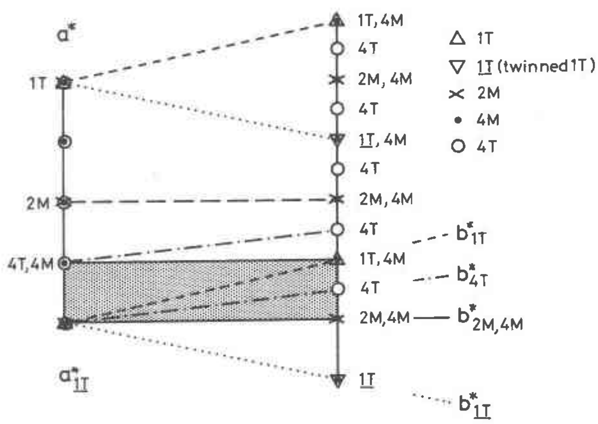

Fig. 4. Relationships of the reciprocal lattice points of 1T, twinned 1T, 2M, 4M and 4T. The shaded area indicates that unit cell of the reciprocal lattice for the 4M polytype. Dotted or broken lines show the respective unit cells.

diffraction intensities could not be measured accurately. The comparison of observed and calculated structure factors, however, confirmed the 4*T* (TTTG) structure, giving an *R* value 0.32 (Table 2), and 0.14 omitting non-observed reflections. The space group is $P\bar{1}$.

The unit cell of the reciprocal lattice for the 4*M* polytype is shown by the shaded area in Figure 4. Note that this figure shows that the arrangement of the reciprocal-lattice points of 2*M*, 1*T* and a twinned equivalent of the latter, with the twofold rotation about *b* as twin operation and (100) as composition plane, simulates that of the 4*M* polytype, thus often giving rise to a misleading interpretation. In the case of the composite crystals of this category, however, the diffraction-intensity distribution varies depending upon the volume ratio of the composite individuals. Therefore, they are readily distinguishable from the distinct 4*M* polytype by a careful observation of the intensity distribution. The "4*T*" polytype reported by Wenk (1969) may be such a case, as has been suggested by Jefferson and Bown (1973). Such an ambiguity remains for a specific composite crystal in which the volume ratio of 2*M*, 1*T* and a twin equivalent of 1*T* is 2:1:1, because such a composite crystal gives *h*10 intensities which are nearly identical with those of the true 4*M* polytype (Table 3).

There are many specimens from Kushiro which give diffraction spots at the same positions as those of 4*M*. Most of these specimens show various intensity distributions obviously different from that of 4*M*. Only 3 out of 56 specimens have been found to give an intensity distribution which is consistent with that of the 4*M* polytype. These crystals, however, may be composite crystals because they break

Table 2. Observed and calculated structure factors of the 4*T* wollastonite

hkl	Fo	Fc	hkl	Fo	Fc
410	0	5.8	$4\bar{1}0$	0	-1.8
510	16	10.8	$5\bar{1}0$	0	2.3
610	5	-6.8	$6\bar{1}0$	0	-4.5
710	12	9.0	$7\bar{1}0$	20	16.5
810	28	-25.3	$8\bar{1}0$	28	21.8
910	28	-25.3	$9\bar{1}0$	12	-10.5
1010	5	8.5	$10\bar{1}0$	12	10.5
1110	3	-5.5	$11\bar{1}0$	24	-20.5
1210	3	6.6	$12\bar{1}0$	16	-13.3
1310	0	1.0	$13\bar{1}0$	0	2.8
1410	0	1.5	$14\bar{1}0$	0	-0.5
1510	0	-3.3	$15\bar{1}0$	0	-3.5
1610	16	11.3	$16\bar{1}0$	5	-8.0
1710	16	11.5	$17\bar{1}0$	3	2.8
1810	0	3.3	$18\bar{1}0$	0	-2.8
430	0	-1.3	$19\bar{1}0$	9	8.3
530	0	3.5			
630	0	2.8	$10\bar{3}0$	0	-0.5
730	0	-0.3	$11\bar{3}0$	0	3.5
830	0	-1.5	$12\bar{3}0$	0	-3.5
930	12	8.5	$13\bar{3}0$	5	6.0
1030	20	15.0	$14\bar{3}0$	28	-21.0
1130	10	-8.5	$15\bar{3}0$	30	-24.5
1230	12	10.3	$16\bar{3}0$	14	10.8
1330	24	-25.3			

Table 3. The calculated structure factors for *h*10 of 4*M* are compared with that of the special composite crystal composed of 2*M*, 1*T* and twinned 1*T* with the domain ratio of 2:1:1 and with *Y* and *Z* directions parallel

4M		2M + 1T + twinned 1T($\underline{1T}$)		
hkl	|Fc|	|Fc|		hkl
010	0	0	2M	010
110	35	35	1T	010
210	40	40	2M	110
310	8	7	$\underline{1T}$	110
410	106	107	2M	210
510	245	249	1T	110
610	420	418	2M	310
710	593	592	$\underline{1T}$	210
810	730	735	2M	410
910	793	792	1T	210
1010	720	715	2M	510
1110	521	523	$\underline{1T}$	310
1210	298	299	2M	610
1310	114	113	1T	310
1410	36	36	2M	710
1510	177	176	$\underline{1T}$	410
1610	301	303	2M	810
1710	364	364	1T	410
1810	313	311	2M	910
1910	176	177	$\underline{1T}$	510
2010	52	53	2M	1010

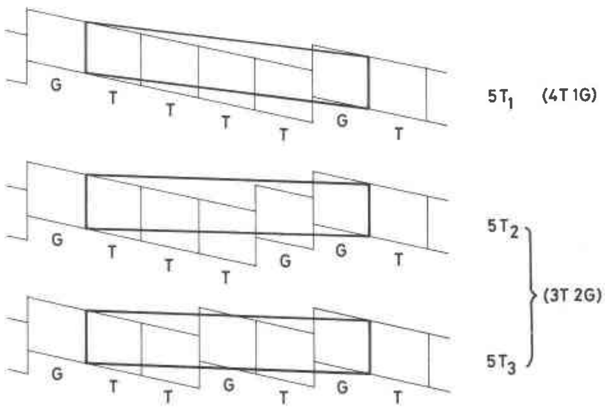

Fig. 5. Three possible stacking sequences for 5*T* polytypes. The unit cells are indicated by thick lines.

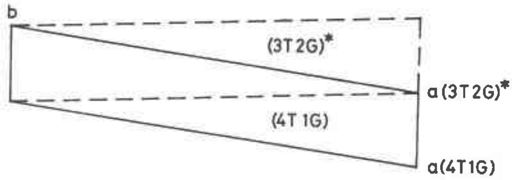

Fig. 6. Relationship of the two cell-types of $5T$ polytypes. The cells are indicated by solid lines for (4T1G) and broken lines for (3T2G)* which is in fact its enantiomorphic equivalent (2T3G).

into fragments giving different intensity distributions.

5T polytypes

As described above, there are three possible stacking sequences for $5T$ polytypes, namely TTTTG (4T1G), TTTGG (3T2G) and TTGTG (3T2G), which may be represented by $5T_1$, $5T_2$ and $5T_3$, respectively (Fig. 5). The relation between the cell types of (4T1G) and (3T2G) types is shown in Figure 6. This metrical relation indicates that the two cell types for the three $5T$ polytypes have lattice points that superpose on the $hk0$ net, and that the indices are related to each other in the following way:

$$hkl_{(4T1G)} = h + k,\ -k,\ l_{(3T2G)}$$

In order to determine the polytype of a specimen, the observed structure factors must be compared with those calculated for each of the three possible polytypes.

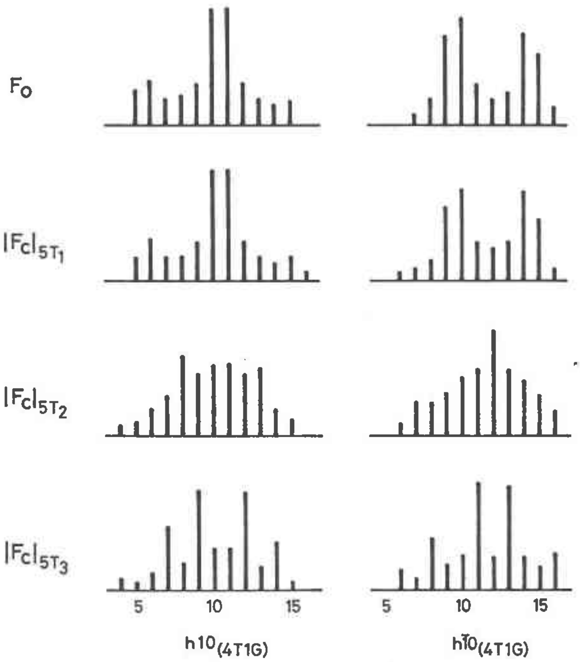

Fig. 7. Comparison between $|F_o|$ and $|F_c|$ for all possible stacking sequences of $5T$ wollastonites.

Only one specimen from Kushiro was found to have a $5T$ polytype. The observed structure factors of the $h10$ reflections are compared in Figure 7 with those calculated for the three possible $5T$ polytypes. The observed values are similar to the calculated values of $5T_1$ (TTTTG or 4T1G). The observed and calculated structure factors of $5T_1$, giving an R value 0.15, are listed in Table 4. $5T_2$ and $5T_3$ give R values 0.67 and 0.86, respectively. The space group for $5T_1$ is $P\bar{1}$.

Lattice constants

The observed lattice constants are compared with the calculated values in Table 5, in which α^*'s (obs.) were assumed to be equal to α^*'s (calc.) because the exact value was not obtained by our X-ray method.

Table 4. Observed and calculated structure factors of the $5T_1$ wollastonite

hkl	Fo	Fc	hkl	Fo	Fc
010	0	0.8	0$\bar{1}$0	0	0.8
110	0	1.4	1$\bar{1}$0	0	0.1
210	0	-0.5	2$\bar{1}$0	0	-0.3
310	0	-0.1	3$\bar{1}$0	0	0.5
410	0	1.0	4$\bar{1}$0	0	-0.3
510	8	-6.1	5$\bar{1}$0	0	1.3
610	10	-10.2	6$\bar{1}$0	0	-1.6
710	6	5.6	7$\bar{1}$0	3	2.5
810	7	-5.9	8$\bar{1}$0	6	4.7
910	10	8.8	9$\bar{1}$0	20	17.0
1010	26	-25.3	10$\bar{1}$0	24	21.1
1110	26	-25.3	11$\bar{1}$0	9	9.4
1210	10	8.4	12$\bar{1}$0	6	7.9
1310	5	-6.5	13$\bar{1}$0	8	-9.1
1410	5	4.2	14$\bar{1}$0	21	19.8
1510	5	-5.9	15$\bar{1}$0	16	13.9
1610	0	-1.6	16$\bar{1}$0	4	-3.2
1710	0	-0.8	17$\bar{1}$0	0	1.1
1810	0	1.8	18$\bar{1}$0	0	0.1
1910	3	-3.5	19$\bar{1}$0	5	-3.9
2010	10	11.3	20$\bar{1}$0	10	-7.4
2110	10	11.6	21$\bar{1}$0	3	4.0
2210	0	-3.5	22$\bar{1}$0	3	-3.6
2310	0	1.8	23$\bar{1}$0	3	4.1
			24$\bar{1}$0	7	-7.7
930	0	0.4	25$\bar{1}$0	2	-3.9
1030	0	-1.9			
1130	8	9.0	7$\bar{3}$0	0	-0.3
1230	16	14.2	8$\bar{3}$0	0	2.0
1330	6	-7.2	9$\bar{3}$0	3	2.8
1430	5	7.1	10$\bar{3}$0	0	-1.3
1530	11	-9.7	11$\bar{3}$0	0	1.0
1630	28	24.8	12$\bar{3}$0	0	-0.9
1730	25	22.3	13$\bar{3}$0	0	0.1
			14$\bar{3}$0	4	-2.9
			15$\bar{3}$0	4	2.6
			16$\bar{3}$0	5	-3.5
			17$\bar{3}$0	6	2.6
			18$\bar{3}$0	24	-21.3
			19$\bar{3}$0	25	-23.9
			20$\bar{3}$0	10	9.8
			21$\bar{3}$0	9	-7.4

Table 5. Cell dimensions of $3T$, $4T$ and $5T_1$ polytypes

	3T		4T		5T	
	calc.	obs.	calc.	obs.	calc.	obs.
$\underline{a}$	23.25 Å	23.2 ± 0.1 Å	31.12 Å	31.2 ± 0.1 Å	38.67 Å	38.6 ± 0.1 Å
$\underline{b}$	7.32	7.30 0.03	7.32	7.30 0.03	7.32	7.30 0.03
$\underline{c}$	7.07	7.06 0.03	7.07	7.06 0.03	7.07	7.06 0.03
α	90.03°	90.0°	90.03°	90.0°	90.03°	90.0°
β	95.50	95.5 ± 0.2°	95.48	95.5 ± 0.2°	95.46	95.5 ± 0.2°
γ	94.51	94.6 0.2	96.75	96.8 0.2	98.09	98.0 0.2

Occurrence of polytypic variants

The skarns of this study were collected at Kushiro, the Town of Tojo, Hiroshima Prefecture, Japan, which is about one kilometer away from the famous outcrop of high-temperature skarn minerals such as gehlenite (Henmi *et al.*, 1971) and spurrite (Kusachi *et al.*, 1971). The mineral assemblage of these skarns is grossular, idocrase, and wollastonite, suggesting that their formation temperatures were distinctly lower than those of the gehlenite-bearing assemblages.

In a crystalline limestone quarry (called Kushiro-Kozan of Kokko-Seifun), zoned skarns with a width of several centimeters occur on both sides of andesite dikes penetrating the crystalline limestone. The skarns are zoned, and the dominant minerals in each zone are as follows:

andesite dike (several centimeters to one meter)
grossular zone (several centimeters)
idocrase zone (zero to one centimeter)
wollastonite zone (zero to several centimeters)
crystalline limestone

Figure 8 shows an example of these zoned skarns.

Wollastonite occurs not only as the main constituent of the wollastonite zone but also as a minor constituent of the grossular and idocrase zones. Wollastonite occurs as acicular aggregates with the long dimension perpendicular to the zone boundaries in the wollastonite zone and also as individual crystals with a short prismatic habit in the grossular and idocrase zones. The wollastonite crystals are largest, up to 1.5 centimeters long, in the wollastonite zone.

The polytypes of wollastonite in each zone were determined by the precession method, with the results as shown in Tables 6 and 7. These tables show that these skarns are zoned with respect to polytypic variants of wollastonite as well as by mineral species. The wollastonite crystals in the wollastonite zone, especially its outer part, are mainly of $1T$ polytype. On the other hand, those in the grossular and idocrase zones are composites of $1T$ and $2M$ polytypes; the volume proportion of $2M$ is usually larger than that of $1T$ in the grossular zone. In general, the volume ratios of $2M$ to $1T$ decrease with increasing distance from the dike. Such a gradual variation continues in the wollastonite zone: the inner part contains crystals which are a composite of $1T$ and $2M$ polytypes but the outer part contains only the $1T$ polytype. For the No. 2 skarn body, the volume ratios of polytypes in each

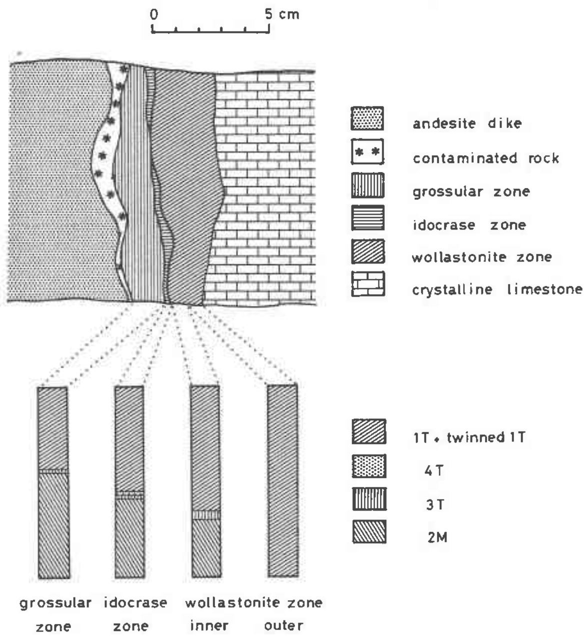

Fig. 8. Cross section through an andesite dike penetrating limestone, showing one side of the contact metasomatic zones (No. 2 skarn). Also shown is the variation of the frequency of the wollastonite polytypes occurring in each zone.

Table 6. The wollastonite polytypes with the mineral assemblage of each zone of No. 2 skarn body

		grossular zone		idocrase zone		wollastonite zone inner		wollastonite zone outer	
width (mm)		8∼15		0∼5		20∼30			
mineral composition		grossular wollastonite idocrase		idocrase wollastonite grossular		wollastonite			
frequency of wollastonite polytypes in each zone	1T	0.0		0.3		0.23		1.0	
	1T,4T	0.0	0.0	0.1	0.4	0.00	0.31	0.0	1.0
	1T,3T	0.0		0.0		0.08		0.0	
	1T>2M	0.1	0.0	0.2	0.2	0.38	0.38	0.0	0.0
	1T,2M	0.4	0.5	0.2	0.3	0.23	0.27	0.0	0.0
	1T,2M,3T	0.1		0.1		0.04		0.0	
	1T<2M	0.3	0.3	0.1	0.1	0.00	0.00	0.0	0.0
	2M	0.1	0.1	0.0	0.0	0.04	0.04	0.0	0.0
	total	1.0		1.0		1.00		1.0	
number of specimens examined		10		10		26		10	

zone were approximately determined by the X-ray intensity measurements and the results are illustrated in Figure 8. Some other skarn bodies (Nos. 10, 11 and 12) also have assemblages which are similar to those of No. 2, but the idocrase zone is absent in No. 10, and only very thin wollastonite zones are contained in some parts of No. 12.

Specimens of 3*T* and 4*T* were found in the No. 2 skarn body. The 3*T* polytype was detected in five specimens from the idocrase zone and its vicinity. These specimens are intimately mixed with 1*T* and 2*M*. A specimen of 4*T* polytype mixed with 1*T* polytype was found also in the idocrase zone. A specimen containing the $5T_1$ polytype mixed with 1*T* was found in the idocrase zone of the No. 12 skarn body.

Discussion

Although wollastonites in gehlenite-bearing skarn bodies at Kushiro are mainly of the 2*M* polytype, those in grossular–idocrase–wollastonite skarns are characterized by the mixtures of 1*T*, 2*M* and others. These polytypic features may be due to the difference in the formation temperatures of the skarns; that is, 2*M* may be regarded as a higher temperature polytype.

Most of the wollastonites in grossular–idocrase–wollastonite skarns are mixtures of 2*M*, 1*T* and twinned equivalents of the latter with *Y* and *Z* directions parallel. There are two kinds of twins, one is related by rotation around [010] and the other by mirror reflection on (100). The domains of the 3*T*, 4*T* and $5T_1$ polytypes are intimately mixed with those of 1*T* and/or 2*M* with the *Y* and *Z* directions parallel. Each polytype frequently is accompanied by disordered stackings on (100). It is noteworthy that the ratios of 2*M* to 1*T* in the zoned skarns decrease gradually with increasing distances from the dike, and that 3*T*, 4*T* and 5*T* polytypes were found only at localities where both 1*T* and 2*M* exist. It is very likely that the long-period polytypes were formed under physical and chemical conditions transitional between those of 1*T* and 2*M*. The polytype transformations have been explained as a result of deformation with shear stress by some workers (Wenk, 1969; Coe, 1970 and Guggenheim, 1978). However, Guggenheim (1978) stated that other processes or a combination of several proc-

Table 7. Wollastonite polytypes in Nos. 2, 10, 11 and 12 zoned skarns

	width of the skarn*	grossular zone	idocrase zone	wollastonite zone inner	wollastonite zone outer
No. 2	30∼50 mm	2M,1T,3T	1T,2M,3T,4T	1T,2M,3T	1T
10	15∼50	——	——	2M,1T	1T
11	5∼15	2M,1T	——	1T	
12	10∼20	1T,2M	1T,2M,5T	1T	

* Sum of the widths of grossular, idocrase and wollastonite zones.

esses may be necessary to produce the periodic faulting. We could not recognize any indication of shear stress at the time of formation of these polytypes at Kushiro, and it is likely that there should be a factor other than a deformation effect that controls polytype formation.

The $3T$ (TTG), $4T$ (TTTG) and $5T_1$ (TTTTG) polytypes from Kushiro consist of several T and only one G stacking in the repeating unit, and their structures may therefore be said to be close to the $1T$ polytype which has no G stacking. This is in contrast with the $7T_8$ polytype (TTGTGTG) from Fuka in that it has the closest structure to $2M$ polytype (TG) among the eight possible $7T$ polytypes (Henmi *et al.*, 1978). The difference may be related to the fact that the Kushiro polytypes occur in $1T$-predominant environments and that Fuka polytype occurs in an aggregate of crystals of the $2M$ polytype.

Acknowledgment

This study was supported by the Grant-in-Aid for Scientific Research from the Ministry of Education, Japan.

References

Bailey, S. W. (1977) Report of the I.M.A.-I.U.Cr. Joint Committee on Nomenclature. American Mineralogist, 62, 411–415.

Buerger, M. J. and Prewitt, C. T. (1961) The crystal structure of wollastonite and pectolite. Proceedings of the National Academy of Sciences of the United States of America, 47, 1884–1888.

Coe, R. S. (1970) The thermodynamic effect of shear stress on the ortho–clino inversion in enstatite and other coherent phase transitions characterized by a finite simple shear. Contributions to Mineralogy and Petrology, 26, 247–264.

Guggenheim, S. (1978) Polytype transformations in experimentally deformed wollastonite. American Mineralogist, 63, 1260–1263.

Henmi, C., Kusachi, I., Kawahara, A., and Henmi, K. (1978) 7T wollastonite from Fuka, Okayama Prefecture. Mineralogical Journal, 9, 169–181.

Henmi, K., Kusachi, I. and Numano, T. (1971) Contact minerals from Kushiro, Hiroshima Prefecture (1) gehlenite and hydrogrossular. Journal of the Mineralogical Society of Japan, 10, 160–169.

Ito, T. (1950) X-ray studies on polymorphism. Maruzen, Tokyo, 93–110.

Jefferson, D. A. and Bown, M. G. (1973) Polytypism and stacking disorder in wollastonite. Nature, Physical Science, 245, 43–44.

Jeffery, J. W. (1953) Unusual X-ray diffraction effects from a crystal of wollastonite. Acta Crystallographica, 6, 821–825.

Kusachi, I., Numano, T., and Henmi, K. (1971) Contact minerals from Kushiro, Hiroshima Prefecture (2) spurrite and tilleyite. Journal of the Mineralogical Society of Japan, 10, 170–180.

Takéuchi, Y. (1971) Polymorphic or polytypic change in biotites, pyroxenes and wollastonite. Journal of the Mineralogical Society of Japan, 10 S, 87–102.

Trojer, F. J. (1968) The crystal structure of parawollastonite. Zeitschrift für Kristallographie, 127, 291–308.

Ueda, T. (1966) Wollastonite and parawollastonite. Tsukumo Earth Science, 1, 11–21.

Wenk, H.-R. (1969) Polymorphism of wollastonite. Contributions to Mineralogy and Petrology, 22, 238–247.

Manuscript received, December 18, 1981; accepted for publication, June 21, 1982.